Lithium Ion Phase-Transfer Reaction at the Interface between the Lithium Manganese Oxide Electrode and the Nonaqueous Electrolyte

Shota Kobayashi*,† and Yoshiharu Uchimoto‡

Nishiki Research Laboratories, Kureha Chemical Industry Co., Ltd, 16, Ochiai, Nishi-machi, Iwaki-city, Fukushima 974-8686, Japan, and Department of Applied Chemistry, Graduate School of Science and Engineering, Tokyo Institute of Technology, 2-12-1 Ookayama, Meguro-ku, Tokyo 152-8552, Japan

Received: December 15, 2004; In Final Form: April 28, 2005

The lithium ion phase-transfer reaction between the spinel lithium manganese oxide electrode and a nonaqueous electrolyte was investigated by the ac impedance spectroscopic method. The dependence of the impedance spectra on the electrochemical potential of the lithium ion in the electrode, the lithium salt concentration in the electrolyte, the kind of solvent, and the measured temperature were examined. Nyquist plots, obtained from the impedance measurements, consist of two semicircles for high and medium frequency and warburg impedance for low frequency, indicating that the reaction process of two main steps for high and medium frequency obey the Butler−Volmer type equation and could be related to the charge-transfer reaction process accompanied with lithium ion phase-transfer at the interface. The dependency on the solvent suggests that both steps in the lithium ion phase-transfer at the electrode/electrolyte interface include the desolvation process and have high activation barriers.

Introduction

Insertion electrode materials have been used in lithium-ion secondary batteries because of their simplicity and high reversibility.[1] The electrochemical charge-transfer reactions proceed with insertion of lithium ions from the electrolyte into the insertion electrode material.

Several researchers have argued that the electrochemical lithium ion insertion process for the lithium-ion secondary batteries involves some reaction steps: diffusion, transfer of lithium ions in the electrolyte bulk, adsorption and conduction of lithium ions on the electrode surface, charge-transfer and desolvation reaction at the electrode/electrolyte interface, diffusion of lithium ions in the electrode bulk, and so forth.[2,3]

Even though many studies have been devoted to the bulk properties of insertion electrodes and electrolyte—especially structural changes of electrodes coupled with lithium insertion and the diffusion or transfer of lithium ions in the electrode or electrolyte bulk, the fundamental mechanism of lithium ion phase-transfer at the interface between the insertion electrode and the nonaqueous electrolyte has not yet been clearly understood; therefore, little is known about charge-transfer and the desolvation process at the electrode/electrolyte interface.

Bruce et al.[4] proposed that the adion model could describe the lithium insertion mechanism at the interface in lithium-ion secondary batteries. They applied the adatom model[5] for the insertion electrode. Figure 1 shows a schematic representation of the proposed adion mechanism for lithium insertion. First, the lithium ion is solvated by several solvent molecules in the electrolyte bulk. Then, the solvated lithium ion in the electrolyte adjacent to the electrode surface loses part of its solvent molecules, and the partially desolvated lithium ion adsorbs on the electrode (formation of the adion); at the same time, electron transfer occurs to preserve electroneutrality. The formed adion diffuses from the electrode surface to a site at which insertion of the lithium ion can occur. In the meantime, a partially desolvated lithium ion loses the remaining solvent molecules and enters into the electrode material. Nakayama et al.[3] interpreted the interfacial reaction process using this adion model as well.

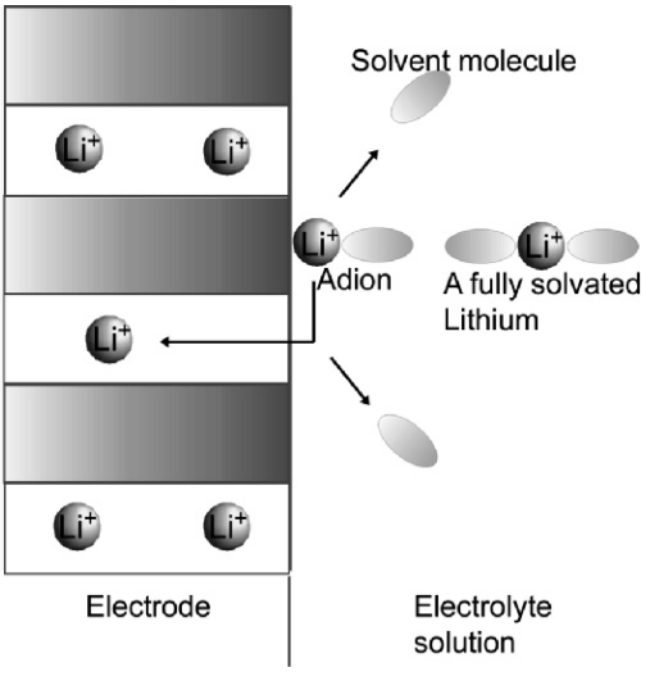

Figure 1. Schematic representation of the lithium intercalation reaction at the electrode/electrolyte interface. (Redrawn from ref 4.)

This study tries to provide evidence for a two-step desolvation reaction in the lithium insertion reaction at the electrode/

* Corresponding author. Tel: +81 246 63 5111. Fax: +81 246 63 7356. E-mail: shota-k@kureha.co.jp.
† Kureha Chemical Industry Co., Ltd.
‡ Tokyo Institute of Technology.

10.1021/jp044283j CCC: $30.25
Published on Web 06/16/2005

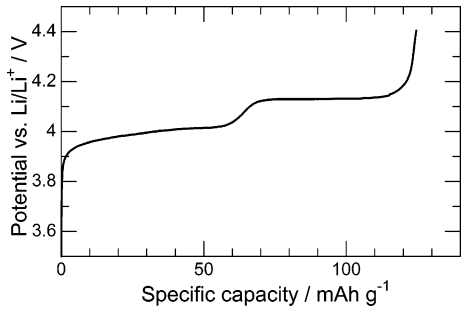

Figure 2. Charge profile obtained with a $LiMn_2O_4$ electrode in PC electrolyte containing 1 mol dm^{-3} $LiClO_4$ at 30 μA cm^{-2}.

electrolyte interface and describes the origin of the impedance components by using an ac impedance method.[6] Electrochemical impedance spectroscopy (EIS) has been well-known as a powerful experimental technique to identify the fundamental mechanism of the lithium ion phase-transfer at the interface between a cathode active material and a nonaqueous electrolyte.[7] We studied the lithium ion insertion mechanism in view of the difference of the solvation energy of the electrolyte. Spinel lithium manganese oxide, one of the most attractive candidates for environmental and economic reasons, was used as the insertion electrode. It also shows a topotactic insertion and extraction of the lithium ion in the 4 V vs Li^+/Li region.[8]

Experimental Details

$LiMn_2O_4$ was synthesized by a conventional solid-state reaction brought about from a stoichiometric mixture of Li_2CO_3 (99.9% Soekawa Chemicals) and Mn_2O_3 (99.9% Kojundo Chemicals) (1:1 mol ratio) at 750 °C for 72 h exposed to air.

Electrochemical characteristics were examined by using a three-electrode electrochemical cell. The working electrodes were prepared by mixing the specimen powder (80 wt %) with carbon black (10 wt %) and polyvinylidine fluoride (10 wt %). Lithium foils were employed as counter and reference electrodes, all of which had constant weight and surface area (1 cm^2). The electrolyte used was 0.1−1 mol dm^{-3} solution of $LiClO_4$ in propylene carbonate (PC), γ-butyrolactone (BL), and dimethyl carbonate (DMC) solution (Tomiyama Pure Chem. Industries LTD). Electrochemical impedance spectroscopic measurements were performed using a frequency response analyzer (Solatron 1255B) and potentio/galvanostat (1287) driven by the Corrware for Windows software (Scribner Associates) at five different temperatures in the range of 5−25 °C. The cell was placed in a thermostatic chamber controlled to the range of ±0.3 °C. Before performing EIS measurements, the potential was changed to 4.0 V and held at the given potential to reach the equilibrium state. The frequency range from 100 kHz to 5 mHz was covered by the impedance spectra with ac amplitude 10 mV. Analysis was made with the measured impedance data, employing a complex nonlinear least-squares fitting program (Z-plot for Windows, Scribner Associates). The electrochemical measurements were carried out galvanostatically at 30 mA cm^{-2} in a glovebox. The cutoff potentials were set at 3.4 V (vs Li^+/Li) and 4.4 V. All the electrochemical experiments were conducted in a glovebox filled with purified argon gas to avoid contact with the air.

Results and Discussion

Figure 2 shows the charge profile obtained with a $LiMn_2O_4$ electrode in PC electrolyte containing 1 mol dm^{-3} $LiClO_4$ at 30 mA cm^{-2}. The electrochemical lithium ion extraction from

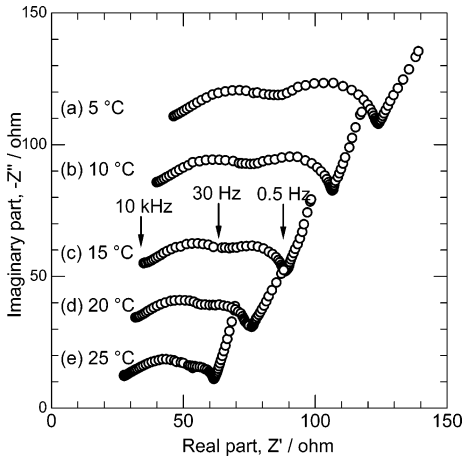

Figure 3. Nyquist plots of the impedance response measured with $LiMn_2O_4$ at 4.0 V in PC electrolyte containing 1 mol dm^{-3} $LiClO_4$ at various temperatures: (a) 5 °C, (b) 5 °C, (c) 15 °C, (d) 20 °C, and (e) 25 °C.

$LiMn_2O_4$ proceeds at about 4 V vs Li^+/Li. The two-plateau figure indicates a phase transition at $Li_{0.5}Mn_2O_4$, which is ascribed to an ordering of lithium on the tetrahedral 8a sites.[9] During charging and discharging in the 4 V potential range, the cubic symmetry of the structure is maintained.[10] However, near 5 V vs Li^+/Li, it is not possible to extract all the lithium ion electrochemically and thus λ-MnO_2 forms.

To investigate the lithium ion insertion mechanism at the electrode/electrolyte interface, EIS were conducted for the $LiMn_2O_4$ electrode during the charge at different temperatures by using various types of lithium salt concentration in the electrolyte. All Nyquist plots obtained from the impedance measurements of $LiMn_2O_4$ consist of two semicircles in the high- and medium-frequency ranges and a thin line at a constant angle inclined to the real axis. Inclination of the line is brought about by the diffusion of the lithium in the $LiMn_2O_4$ bulk.[11] Two semicircles were observed in the range of 50 kHz to 0.1 Hz. Hereafter, semicircles for high and medium frequency will be defined as semicircle 1 and semicircle 2, respectively. To confirm the influence of the storage time at 4.0 V vs Li^+/Li, we carried out the following measurements. The electrode was charged up to 4.0 V and held at this level. EIS measurements were then performed intermittently for up to 170 h. The size of the semicircle is not observed to increase with increasing the storage time under our experimental condition. We show the Nyquist plots of the impedance response measured with $LiMn_2O_4$ at 4.0 V in PC electrolyte containing 1 mol dm^{-3} $LiClO_4$ at various temperatures (Figure 3). In general, the absolute impedance decreases markedly with increasing temperature. It is difficult to estimate the accurate value of each resistance at 30 °C or more because two semicircles become inseparable because of the effect of the relative time constants under our experimental conditions.

The impedance of the electrode can be interpreted in terms of a simple circuit in which a resistance−capacitance network is connected in series with the bulk resistance of the electrolyte. To evaluate each resistance, the nonlinear least-squares fitting program was applied within the measured frequency region. Analysis was made with respect to the impedance spectra using a simple equivalent circuit generally applicable to the lithium transition metal oxide for cathode materials. Figure 4 illustrates the equivalent circuit model used to analyze the experimentally obtained impedance spectra. R_s represents the electrolyte resistance. R_1 and R_2 represent the resistance for high and

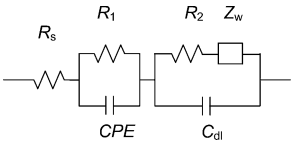

Figure 4. Equivalent circuit model used to analyze the obtained impedance spectra. R_s represents the electrolyte resistance, R_1 and R_2 represent the resistance for high and medium frequency, respectively, C_2 is the capacitance, and Z_W is the Warburg impedance.

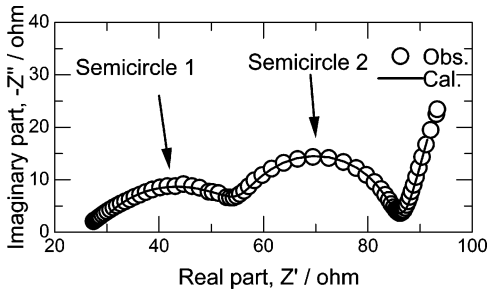

Figure 5. Typical Nyquist plot and the corresponding result of curve-fitting. These data were observed at 4.125 V, 25 °C. The electrolyte was a 1 mol dm^{-3} solution of $LiClO_4$ in PC.

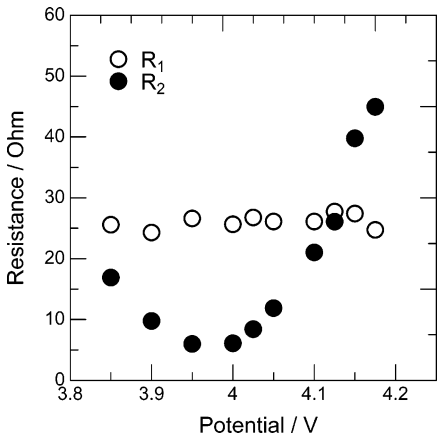

Figure 6. Plots of R_1 and R_2 determined by using the nonlinear least-squares fitting program as a function of the electrode potential for $LiMn_2O_4$ in PC electrolyte containing 1 mol dm^{-3} $LiClO_4$ at 25 °C.

medium frequency, respectively. C_2 is the capacitance, and Z_W is the Warburg impedance. To account for the depression of the high-frequency semicircle, a constant phase element[12] (CPE) was utilized in place of the capacitor in this model. The CPE is commonly used to describe the depressed semicircle that results from a porous electrode.

A typical Nyquist plot is presented with the corresponding result of curve-fitting in Figure 5. The χ^2-value of the fit was low (the order of 10^{-4} to 10^{-6}), and the curve-fitting results were in good agreement with the actual measurement value (see Figure 5). Figure 6 shows plots of R_1 and R_2 determined by using the nonlinear least-squares fitting program as a function of the electrode potential for $LiMn_2O_4$ in PC electrolyte containing 1 mol dm^{-3} $LiClO_4$ at 25 °C. R_2 is strongly dependent on the electrode potential, while change of R_1 is flatter than that of R_2.

Generally, the charge-transfer reaction at the electrode/electrolyte interface could be determined from the rearranged Butler−Volmer equation.[6] According to the Butler−Volmer equation, exchange current density i_0 is expressed as follows:

$$i_0 = A(C_O)^{1-\alpha}(C_R)^{\alpha}\exp\left(\frac{-\Delta G^*}{RT}\right) \quad (1)$$

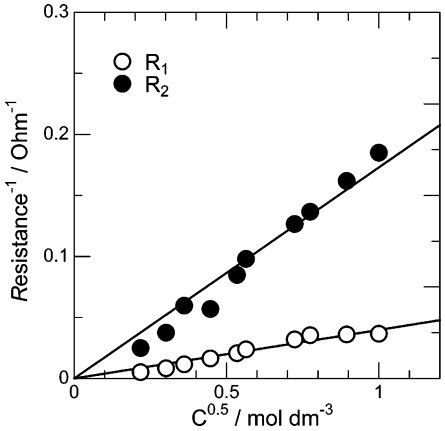

Figure 7. Plots of inverse R_1 and R_2 at 4.0 V (vs Li^+/Li) vs the square root of lithium salt concentrations in electrolyte for $LiMn_2O_4$ at 25 °C. The electrolyte was a 0.1−1 mol dm^{-3} solution of $LiClO_4$ in PC.

where A is the preexponential factor, $(C_O)^{1-\alpha}$ and $(C_R)^{\alpha}$ are the activities of lithium in the electrolyte and electrode, respectively, and α and ΔG^* are the transfer coefficient and the Gibbs free energy of activation, respectively. R is the gas constant, and T is the absolute temperature. It has been known that the charge-transfer resistance (hereafter referred to as R_{ct}) is related to the exchange current density by the following equation:[6]

$$i_0 \propto \frac{1}{R_{ct}} = \left(\frac{nFi_0}{RT}\right) \quad (2)$$

where F is Faraday's constant.

Since the impedance measurements were conducted on the constant electrode potential, assuming that $(C_R)^{\alpha}$ is constant, eqs 1 and 2 lead to the following expression:

$$\frac{1}{R_{ct}} \propto i_0 = A(C_O)^{\alpha}\exp\left(\frac{-\Delta G^*}{RT}\right) \quad (3)$$

The above equation has the consequence that inverse charge-transfer resistance, R_{ct}^{-1}, is proportional to the lithium salt concentration in the electrolyte, C_O^{α}. Figure 7 depicts the plots of inverse R_1 and R_2 at 4.0 V (vs Li^+/Li) vs lithium salt concentrations in the electrolyte for $LiMn_2O_4$. As shown in Figure 7, inverse R_1 and R_2 are linearly proportional to the lithium salt concentration in the electrolyte to the one-half power. Therefore, each transfer coefficients, α, is 0.5. The result from Figure 7 showed that the obtained R_1 and R_2 values support the Butler−Volmer equation for all lithium concentrations in the electrolyte. Accordingly, two physical phenomena (semicircles 1 and 2) occurred during lithium ion phase-transfer at the electrode/electrolyte interface and could be described as the charge-transfer process related to the lithium ion at the interface.

Since R_1 for semicircle 1 and R_2 for semicircle 2 obeyed the Butler−Volmer type equation, the activation energy for each process was evaluated from eq 3. The lithium ion is strongly coordinated by solvent molecules in the electrolyte. It already has been shown by nuclear magnetic resonance (NMR) measurement that inserted lithium exists as charged Li^+ ions in the host lattice.[14] As energy is needed to desolvate solvent molecules in the lithium ion phase-transfer process, this requirement must lead to an activation barrier. Figure 8 shows plots of $\ln(R_1^{-1})$ vs inverse temperature for the $LiMn_2O_4$ electrode in different solvents. Propylene carbonate, γ-butyrolactone, and dimethyl carbonate were used as solvents, and are hereafter abbreviated as PC, BL, and DMC, respectively. Plots of $\ln(R_1^{-1})$ against

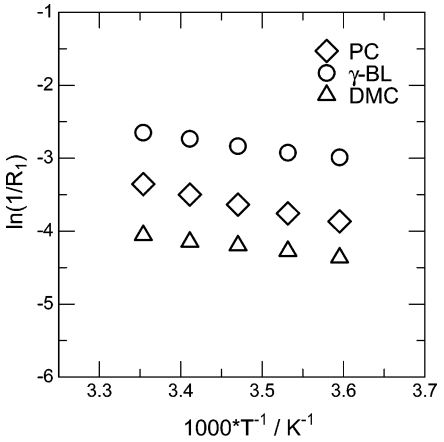

Figure 8. Plots of $\ln(R_1^{-1})$ vs inverse temperature for the $LiMn_2O_4$ electrode in different solvents.

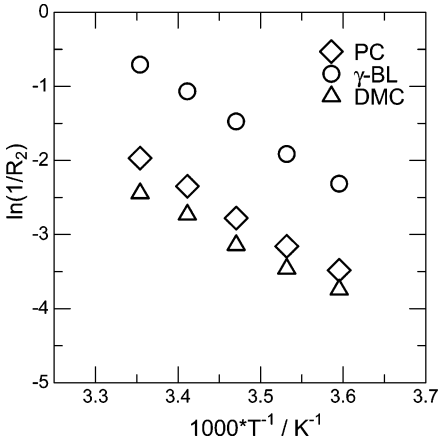

Figure 9. Plots of $\ln(R_2^{-1})$ vs inverse temperature for the $LiMn_2O_4$ electrode in different solvents.

$10^3 \times T^{-1}$ for $LiMn_2O_4$ electrodes were found to be linear; therefore, the Arrhenius equation is considered to be valid. The activation energies for the charge-transfer process at 4.0 V were determined experimentally from the slope of $\ln(R_{ct}^{-1})$ vs $10^3 \times T^{-1}$ plot. The activation energy of the process for semicircle 1, represented by E_1, exhibited solvent dependency. Activation energies for R_1 were in the order of PC (19 kJ mol^{-1}) > BL (15 kJ mol^{-1}) > DMC (10 kJ mol^{-1}). This result shows that the charge-transfer process for semicircle 1 at the electrode/electrolyte interface involves the desolvation reaction process. The desolvation reaction of the lithium ion inevitably affects the lithium ion transfer kinetics at the electrode/electrolyte interface.

Figure 9 shows plots of $\ln(R_2^{-1})$ vs the inverse temperature for the $LiMn_2O_4$ electrode with different solvents. Activation energy of the process for semicircle 2, represented by E_2, also exhibited solvent dependency. The results of activation energies for R_1 and R_2, E_1 and E_2, appear in Table 1. The effect of the solvent in Figures 8 and 9 indicates that both steps of the lithium ion phase-transfer at the electrode/electrolyte interface include the desolvation process. Therefore, the desolvation process at the electrode/electrolyte interface proceeds by way of two main steps, partial desolvation, and the loss of remaining solvent. These results show good agreement with the adion mechanism proposed by Bruce et al.

As shown in Figure 6, resistance R_1 for semicircle 1 was imperceptible changed for the electrochemical potential of the lithium ion in the electrode. Considering the electrode potential dependency for R_1, the reaction process for semicircle 1 could be regarded as the partial desolvation reaction of lithium ions and the adion formation reaction at the electrode/electrolyte interface. In the meantime, resistance R_2 for semicircle 2 strongly depends on the electrochemical potential of the lithium ion in the electrode. Taking the electrode potential dependency for R_2 into consideration, the reaction process for semicircle 2 is the diffusion of the partially desolvated lithium ion on the electrode surface, a reaction in which a partially desolvated lithium ion loses the remaining solvent molecules, and an incorporation reaction of lithium ion into the host lattice. It is therefore clear that the lithium ion phase-transfer reaction at the electrode/electrolyte interface involves a two-step desolvation reaction.

TABLE 1: Activation Energies for R_1 and R_2, E_1 and E_2, at 4.0 V (vs Li^+/Li)[a]

	activation energy (kJ mol^{-1})	
solvent	semicircle 1 (E_1)	semicircle 2 (E_2)
PC	19	54
BL	15	53
DMC	10	48

[a] The electrolyte was a 1 mol dm^{-3} solution of $LiClO_4$ in propylene carbonate (PC), γ-butyrolactone (BL), and dimethyl carbonate (DMC) solution.

The energy related to the desolvation of the lithium ion can be estimated by the solvation energy of the lithium ion. The solvation of the lithium ion is dependent on the energies of the Li^+-O bond and the interactions among solvent molecules as they solvate the ion. A detailed understanding of these interactions can be achieved thorough quantitative and computational studies of the salvation energies in the gas phase.[15,16] Klassen et al.[16] have reported the binding energies of the various solvents to the lithium ion. The solvation energies calculated by ab initio calculations using the HF/6-311++G** basis set were −199.4 kJ mol^{-1} (PC) and −190.4 kJ mol^{-1} (DMC). However, we cannot compare simply the absolute calculated value and the absolute experimental value because the calculated value is based on some hypothesis (for example, the solvation energies are estimated high because the bare lithium ion is unstable in the gas phase). Even so, the calculated solvation energies are given by the order of PC > DMC. Experimental results showed good agreement with the tendency of theoretical calculation. The activation energies for the lithium ion phase-transfer reaction at the electrode/electrolyte interface are greatly influenced by the interaction between the lithium ion and solvents.

The solvated lithium ion considered in the primary solvation shell of the cation were $Li^+(solvent)_n$ ($n = 1-4$) based on the results of Hyodo et al.[17] and Izutsu et al.[18] However, the absolute values for the solvation number are slightly different from each other. The primary solvation number of the lithium ion in some organic solvents in the electrolyte was shown to be four. Consequently, it seems that several solvent molecules in four solvent molecules desolvate from the lithium ion in reaction process 1 (formation of adion), and the remaining solvent molecules desolvate from the lithium ion in reaction process 2. A schematic representation of the lithium ion phase-transfer reaction mechanism under the obtained results is illustrated in Figure 10. A high activation barrier existed at the lithium manganese oxide electrode/ nonaqueous electrolyte interface for the lithium ion transfer process. The activation barrier is greatly influenced by the lithium ion−solvents interaction.

Conclusions

On the basis of the adion model proposed by Bruce et al., the lithium ion phase-transfer reaction at $LiMn_2O_4$ electrode/

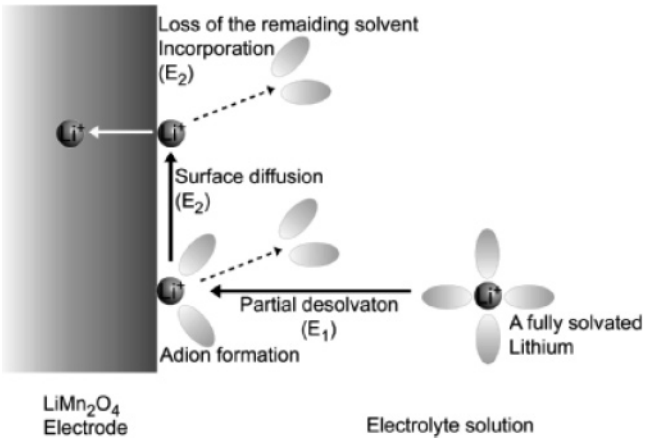

Figure 10. Schematic representation of the lithium ion phase-transfer reaction mechanism.

nonaqueous electrolyte interface was studied in view of differences of the solvation energy of the electrolyte. Electrochemical impedance spectroscopy (EIS) measurements under various conditions revealed the origin of physical phenomena at the electrode/electrolyte interface. Our EIS results show that the lithium ion phase-transfer reaction has two main steps and includes the desolvation reaction. The desolvation reaction of lithium ion occurred simultaneously with the charge-transfer process on the electrolyte side. One reaction process for semicircle 1 was the partial desolvation reaction of lithium ions and the adion formation reaction on the electrode surface. The other reaction process for semicircle 2 was adsorption and a diffusion reaction of a partially desolvated lithium ion on the electrode surface, a reaction in which a partially desolvated lithium ion loses the remaining solvent molecules, and an incorporation reaction of the lithium ion into the host lattice.

Acknowledgment. This work was supported by Grant-in Aid for Scientific Research on Priority Area (B) (No. 740) "Fundamental Studies for Fabrication of All Solid State Ionic Devices" from Ministry of Education, Culture, Sports, Science and Technology.

References and Notes

(1) (a) Scrosati, B. *Nature* **1995**, *373*, 557. (b) Tarascon, J.-M.; Armand, M. *Nature* **2001**, *414*, 359.

(2) Dokko, K.; Mohamedi, M.; Umeda, M.; Uchida, I. *J. Electrochem. Soc*. **2003**, *150*, A425.

(3) Nakayama, M.; Ikuta, H.; Uchimoto, Y.; Wakihara, M. *J. Phys. Chem. B* **2003**, *107*, 10603.

(4) (a) Bruce, P. G.; Saidi, M. Y. *J. Electroanal. Chem*. **1992**, *322*, 93. (b) Bruce, P. G.; Saidi, M. Y. *Solid State Ionics* **1992**, *51*, 187.

(5) Despic, A. R.; Bockris, J. O'M. *J. Chem. Phys.* **1960**, *32*, 389.

(6) Bard, A. J.; Faulkner, L. R. *Electrochemcal Methods. Fundamentals and Applications*; John Wiley & Sons: New York, 1980; pp 87−136.

(7) (a) Levi, M. D.; Salitra, G.; Markovsky, B.; Teller, H.; Aurbach, D.; Heider, U.; Heider L. *J. Electrochem. Soc.* **1999**, *146*, 1279. (b) Dokko, K.; Mohamedi, M.; Fujita, Y.; Itoh, T.; Nishizawa, M.; Umeda, M.; Uchida, I. *J. Electrochem. Soc*. **2001**, *148*, A422. (c) Nobili, F.; Tossici, R.; Marassi, R. *J. Phys. Chem. B* **2002**, *106*, 3909. (d) Choi, Y.-M.; Pyun, S.-I.; Bae, J.-S.; Moon, S.-I. *J. Power Sources* **1995**, *56*, 25. (e) Hjelm, A.-K.; Lindbergh, G. *Electrochem. Acta* **2002**, *47*, 1747.

(8) (a) Guyomard, D.; Tarascon, J. M. *Solid State Ionics* **1994** *69*, 222. (b) Gummow, R. J.; Kock, A. de; Thackeray, M. M. *Solid State Ionics* **1994**, *69*, 59. (c) Tarascon, J. M.; McKinnon, W. R.; Coowar, F.; Bowmer, T. N.; Amatucci, G.; Guyomard, D. *J. Electrochem. Soc*. **1994**, *141*, 1421. (d) Gao, Y.; Dahn, J. R. *J. Electrochem. Soc*. **1996**, *142*, 100.

(9) Goodenough, J. B.; Thackeray, M. M.; David, W. I. F.; Bruce, P. G. *Rev. Chim. Miner*. **1984**, *21*, 435.

(10) (a) Ohzuku, T.; Kitagawa, M.; Hirai, T. *J. Electrochem. Soc*. **1990**, *137*, 769. (b) David, W. I. F.; Thackeray, M. M.; Picciotto, L. A.; Goodenough, J. B. *J. Solid State Chem.* **1987**, *67*, 316.

(11) Ho, C.; Raistrick, I. D.; Huggins, R. A. *J. Electrochem. Soc.* **1999**, *127*, 343.

(12) *Impedance Spectroscopy, Emphasizeng Solid Materials and Systems*; Madonald, J. R., Ed.; Wiley & Sons: New York, 1987.

(13) Mohamedi, M.; Takahashi, D.; Ishizawa, M. *J. Power Sources* **1999**, *81*−*82*, 425.

(14) Sibernagel, B. G.; Whittingham, M. S. *J. Chem. Phys*. **1976**, *64*, 3670.

(15) (a) Wang, Y.; Balbuena, P. B. *J. Phys. Chem. B* **2002**, *106*, 4486. (b) Yanase, S.; Oi, T. *J. Nucl. Sci. Technol.* **2002**, *39*, 1060. (c) Marcus, Y. *Ion solvation*; Wiley: Chichester, 1985; p 72.

(16) Klassen, B.; Aroca, R.; Nazri, M.; Nazri, G. A. *J. Phys. Chem. B* **1998**, *102*, 4795.

(17) Hyodo, S.; Okabayashi, K. *Electrochem. Acta* **1989**, *34*, 1551.

(18) Izutsu, K.; Nakamura, T.; Miyoshi, K.; Kurita, K. *Electrochem. Acta* **1996**, *41*, 2523.